Channel Precoding for Indoor Radio Communications Using Dimension Partitioning

Yuk-Lun Chan and Weihua Zhuang, *Member, IEEE*

***Abstract*— In this paper, a new phase precoding technique is developed to combat the intersymbol interference (ISI) resulting from a frequency-selective slowly fading channel in a personal communication system using quadrature phase-shift keying (QPSK). Based on a new dimension partitioning technique, the precoder predistorts only the phase of the transmitted signal to keep a constant transmitted signal amplitude and, therefore, to ensure the stability of the precoder even in equalizing a nonminimum-phase channel. Under the constraint of the constant amplitude, the dimension partitioning method is developed to guarantee the possibility of correct detection for all transmitted information symbols and to further improve the transmission accuracy by increasing the size of decision regions. Analytical and simulation results demonstrate that over frequency-selective Rayleigh and Rician fading channels, the system using the proposed channel precoder can achieve a bit error rate (BER) comparable with that using a conventional decision feedback equalizer (DFE). The precoder can outperform DFE in an indoor environment where there is a strong direct propagation path. The main advantage of using the precoder is that the impairment of ISI due to multipath propagation on the transmission performance can be mitigated without increasing the complexity of the portable unit receiver. The proposed technique is especially useful for personal communications, where ISI due to multipath fading channels can severely deteriorate the BER transmission performance and where the simplicity of portable units is a vital characteristic of the system.**

***Index Terms*— Channel precoding, dimension partitioning, equalization, frequency-selective fading, indoor wireless communications.**

I. Introduction

IN AN INDOOR wireless communication system, due to reflection, refraction, and scattering, transmitted signals often arrive at the receiver through more than one path. The multipath propagation introduces fading and delay spread to the transmitted signals. At a high-transmission rate, the delay spread results in intersymbol interference (ISI) which can significantly degrade the transmission performance [1]. Channel equalization is an efficient approach to combating the effect of ISI, and decision feedback equalizer (DFE) is the most popular nonlinear equalizer for severe fading channels [2], [3]. However, when coded modulation is used to further improve system performance, the straightforward combination of coding with a DFE may not perform well because zero-delay decisions in a coded system are not sufficiently reliable for decision feedback. The problem can be solved at the expense of receiver complexity, such as using parallel decision feedback decoding (PDFD) which puts the DFE function inside a Viterbi decoder [4], [5]. The PDFD technique uses a unique sequence of decisions for each state in the trellis, rather than using only one sequence of decisions in the feedback path of the DFE. These feedback sequences are based on the history of each state's surviving path. As a result, instead of calculating metrics with one received sample per trellis stage, it is necessary to calculate metrics with a unique decision feedback sample for each state at that stage. Such approaches are in conflict with desirable characteristics of portable units of low-power personal communication systems. A key requirement for such systems is the availability of compact light handheld portable voice and data units. Portable units are battery powered and have stringent power and size constraints. On the other hand, the constraints are not so severe at the base stations. These considerations lead to the approach of moving channel equalization functions from the receiver of a portable unit to the transmitter of the base station, so that the portable unit can be relieved from equalization tasks.

If the channel characteristics are known to the base-station transmitter, channel precoding (or preequalization) becomes possible for the forward link from the base station to the portable unit. Unlike a DFE which performs channel equalization at the receiver, precoding is a transmitter technique. Ideally, the transfer function of the precoder is the inverse of the channel transfer function. However, when the fading channel is not minimum phase, the inverse of the channel transfer function is unstable, which means that we cannot have a linear and stable channel precoder. Nonlinear operation is necessary to achieve the precoder stability. The main challenge of implementing such a precoder is to ensure its stability even in equalizing a nonminimum phase fading channel and, at the same time, to achieve an ISI-free received signal. Furthermore, when phase modulation is used, a constant transmitted signal amplitude is usually preferred. This extra constraint makes the development of channel precoding techniques even more complex. Tomlinson–Harashima (TH) precoding is a technique very suitable for quadrature amplitude modulation (QAM) [6], [7]. The key point in TH precoding is the nonlinear modulo-arithmetic operation to guarantee the stability of the precoder. However, TH precoding cannot be directly applied to time-varying fading channels where amplitude fading causes severe errors in retrieving the original

Manuscript received December 15, 1995; revised October 28, 1996. This work was supported by the Natural Sciences and Engineering Research Council (NSERC) of Canada under Grant OGP0155131.

Y.-L. Chan is with the Symantec Corporation, Toronto, Ont., M3C 1W3, Canada.

W. Zhuang is with the Department of Electrical and Computer Engineering, University of Waterloo, Waterloo, Ont., N2L 3G1, Canada.

Publisher Item Identifier S 0018-9545(99)00603-9.

amplitude information at the receiver, due to the corresponding modulo-arithmetic reduction. Furthermore, TH precoding is undesirable for phase modulation with constant amplitude because after TH precoding, the signal no longer has a constant amplitude. Phase modulation such as phase-shift keying (PSK) is usually preferred in personal communication systems due to its frequency spectral efficiency. Using PSK, it is desired to have a constant precoded signal amplitude, even though in practice pulse shaping is commonly used to meet out-of-band spectral emission requirements. This can be explained as follows. Pulse shaping after precoding results in fluctuations of the envelope of the transmitted signal. When the time varying envelope of the precoded and filtered signal is amplified by a nonlinear power-efficient output amplifier, signal distortions occur and transmission performance degrades. If the precoder keeps a constant signal amplitude, then the envelope variations at the amplifier input are solely due to pulse shaping and therefore are smaller than those when TH precoding is used (since TH precoding introduces extra envelope variations). Indeed, it is possible that the envelope fluctuations introduced by precoding can dominate that introduced by pulse shaping. In the case that a linear power amplifier is used, a precoder without the constraint of a constant signal amplitude introduces energy dispersion (on frequency domain) to the transmitted signal. The dispersion is time-varying and depends on the ISI component at the instant. With a filter for pulse shaping at the transmitter and a matched filter at the receiver for signal detection, the signal distortion due to the dispersion cannot be remedied due to its random nature. As a result, under the same channel condition and the same spectral efficiency, a precoded PSK signal with a constant amplitude can achieve a required bit error rate (BER) with a smaller transmitted signal power than one without a constant amplitude.

Recently, an adaptive channel precoding technique has been proposed for phase modulation over a slowly fading channel [8]. An automatic gain control (AGC) unit is used in the adaptive precoder to achieve a constant amplitude. However, the AGC unit also introduces nonlinear distortion to the precoded signal and results in channel equalization errors. In order to reduce the equalization error, another precoding method intended for M-ary PSK (MPSK) has been proposed in [9], which establishes a relationship between the phase and amplitude of the received signal by a spiral curve design. By adaptively choosing the spiral curve according to channel fading status, the precoding method can keep a constant transmitted signal amplitude, stabilize the precoder, and ensure ISI-free transmission. Different from the approach given in [9], in this paper a novel channel precoding technique is proposed for a time-division multiple-access (TDMA) indoor radio system operating in a time-division duplex (TDD) mode using quaternary PSK (QPSK). The precoding technique is developed based on a new dimension partitioning technique. With the proposed technique, only the carrier phase is predistorted so that the precoded signal amplitude can be kept constant. As a result, the proposed precoding technique overcomes the drawbacks of TH precoding. The advantages of the newly proposed precoding technique are that: 1) ISI-free transmission can be achieved without increasing the complexity of portable units; 2) the frequency spectrum in wireless communications can be utilized more efficiently as compared with that of the conventional 2×2 QAM using TH precoding; 3) the precoder is always stable; and 4) there is no error propagation problem. The performance of the precoding technique is analyzed theoretically and verified by computer simulations. The numerical results confirm that the system using the proposed channel precoder can achieve a BER comparable with that using a conventional DFE. When there is a strong direct propagation path, the precoder can outperform a DFE which suffers from error propagation. This paper is organized as follows. Section II describes the communication system structure where the precoder is used. In Section III, the principles and operations of the newly proposed channel precoding technique are presented. The transmission performance of the system using the proposed precoding technique is analyzed theoretically in Section IV. Numerical analysis results and computer simulation results of the transmission performance are presented and discussed in Section V. Section VI gives the conclusions of this work.

II. System Description

Fig. 1 shows the functional block diagram of a TDMA/TDD indoor wireless communication system with asymmetric channel equalization. For simplicity, it shows only one base station and one portable unit linked by a radio channel. In the reverse link from the portable unit to the base station, a DFE is used to reduce the ISI resulting from the fading channel. The channel estimator estimates the channel impulse response based on the tap coefficients of the DFE. In the system operating in a TDD mode, both forward link and reverse link share the same radio channel by using different time slots. If the channel impulse response is time invariant, i.e., the channel can be modeled as a linear time-invariant system, then the radio frequency (RF) links are reciprocal according to the reciprocity theorem applied to radiation patterns and linear systems [10], [11]. In the case that the radio channel impulse response is time variant, if the channel fades so slowly that the channel characteristics are approximately invariant over the time interval of two adjacent data frames for the forward and reverse links, respectively, then the RF links are reciprocal over the time interval of the two adjacent data frames. As a result, the channel information estimated in the reverse link can be used in the precoder at the base-station transmitter to preequalize the signal transmitted in the forward link. With the channel precoding, the signal received at the portable unit is ISI free. Since all the channel equalization functions are performed at the base station, the simplicity of the portable unit can be obtained.

The time-variant frequency-selective fading channel can be described by its complex impulse response at baseband [12]–[14]

$$h(t) = \sum_{k=0}^{K} \alpha_k(t) e^{j\phi_k(t)} \delta(t - \tau_k) \tag{1}$$

where K is the number of the delayed paths, $\alpha_k(t), \phi_k(t)$, and τ_k are the amplitude fluctuation, carrier phase jitter,

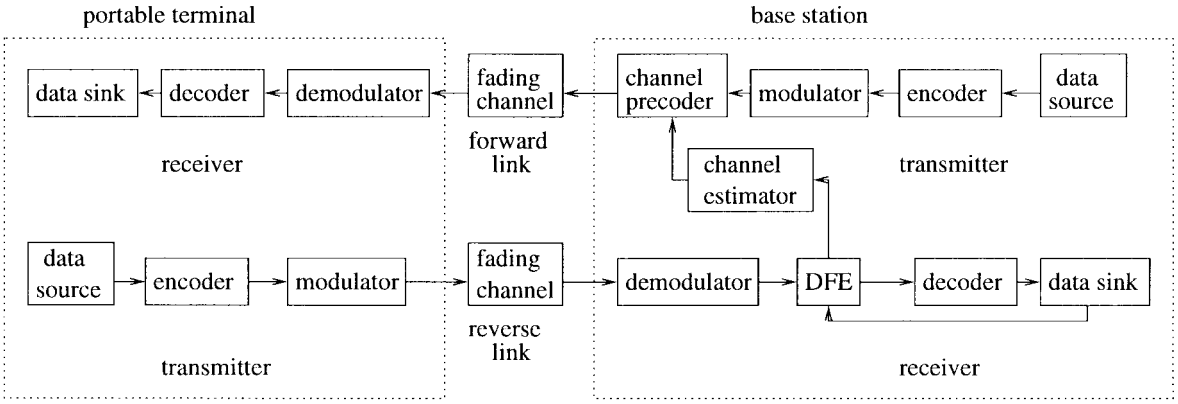

Fig. 1. Functional block diagram of system model.

and propagation delay of the kth path, respectively. Usually, $\alpha_0(t)$ is Rician distributed or Rayleigh distributed, depending on whether there is a line-of-sight (LOS) path or not, and $\alpha_k(t)$ $(k>0)$ is Rayleigh distributed with $\phi_k(t)$ being uniformly distributed over $[0, 2\pi]$. In addition to experiencing fading and dispersion, the received signal is also contaminated by additive white Gaussian noise (AWGN).

QPSK with both absolute phase encoding and differentially encoding [15] is considered here. In considering frequency reuse in indoor radio systems, four-level phase modulation is the most spectrally efficient for the portable environment [16]. Although QPSK is similar to 2 × 2 QAM, there is one distinction between them when the binary waveforms are filtered before modulating the signals. In QPSK, the filtered waveform is applied to a phase modulator resulting in a constant envelope signal with a reduced phase transition rate determined by the filtering. In 2 × 2 QAM, the filtered waveforms amplitude-modulate the two quadrature signals. Thus, the resulting sum of the quadrature signals not only has a reduced phase transition rate, but also has amplitude variations, i.e., it is not constant envelope. In the following, we focus on the new channel precoding for QPSK instead of 2 × 2 QAM. The signal to be transmitted over the ith symbol interval $[iT, iT+T]$ can be represented by its complex-valued amplitude denoted as $d_i = Ae^{j\beta_i}$, where T is the symbol interval, A is the constant transmitted signal amplitude, and β_i can take on values of $\pi/4,\ 3\pi/4,\ 5\pi/4$, or $7\pi/4$ representing the transmitted information. The corresponding precoded signal is $s_i = Ae^{j\theta_i}$. As explained earlier, a constant amplitude A is desired for the precoded signal although a filter for pulse shaping implemented after the precoder can introduce envelope fluctuations to the transmitted signal.

III. Precoding Using Dimension Partitioning

In the following, the new precoding method based on the idea of dimension partitioning is developed for QPSK [17]. Using this precoding scheme, the precoded signal has a constant amplitude and the decision regions are larger than those of TH precoding, so that the drawbacks of TH precoding can be mitigated. For completeness, TH precoding is first reviewed and is interpreted from a new point of view—using the concept of dimension partitioning.

A. TH Precoding

TH precoding was proposed for QAM. Here, we consider a conventional $L \times L$ QAM, where the modulo-arithmetic operation (with parameter $2L$) is performed on both in-phase and quadrature components of the signal. For a slowly fading channel, the channel impulse response is approximately time invariant over each symbol interval. If $\tau_k = kT$, then the channel impulse response (1) over $t \in [iT, iT+T]$ can be simplified to

$$h(t) = \sum_{k=0}^{K} h_k \delta(t - kT) \tag{2}$$

where $h_k = \alpha_k(iT)e^{j\phi_k(iT)}$. In the case that $h_0 = 1$, if the desired received sample at $t = iT + T$ is d_i at baseband and the corresponding ISI is $I_i = \Sigma_{k=1}^{K} h_k x_{i-k}$ (where x_{i-k} is the previously transmitted signals at baseband), then ISI-free transmission can be achieved by transmitting (equivalent signal at baseband)

$$x_i = d_i - I_i. \tag{3}$$

The operation of the precoder is then to map the desired signal d_i to the transmitted signal x_i, which can be described by the transfer function of the precoder

$$\frac{X(z)}{D(z)} = \frac{1}{1 + [H(z) - 1]} = H^{-1}(z) \tag{4}$$

where $H(z) = \Sigma_{k=0}^{K} h_k z^{-k}$ is the channel transfer function. As long as $H(z)$ has all its zeros inside the unit circle of the complex z plane, $H^{-1}(z)$ is stable and so is the precoder. However, if the channel is not minimum phase, the above condition is no longer valid and the precoder becomes unstable. The sequence $\{x_i\}$ will tend to increase or diverge indefinitely. In order to stabilize the precoder, TH precoding uses a nonlinear modulo-arithmetic operation. Fig. 2 shows the structure of a TH precoding system. The precoder is basically an inverse filter $H^{-1}(z)$ of the channel transfer function $H(z)$, except that the output of the filter undergoes modulo-arithmetic operation before being transmitted and being applied back to the feedback filter. That is, in order to achieve stability, the TH precoder sends (instead of $x_i = d_i - I_i$)

$$x_i' = [(d_i - I_i) \bmod 2L] = d_i + 2Lk_i - I_i \tag{5}$$

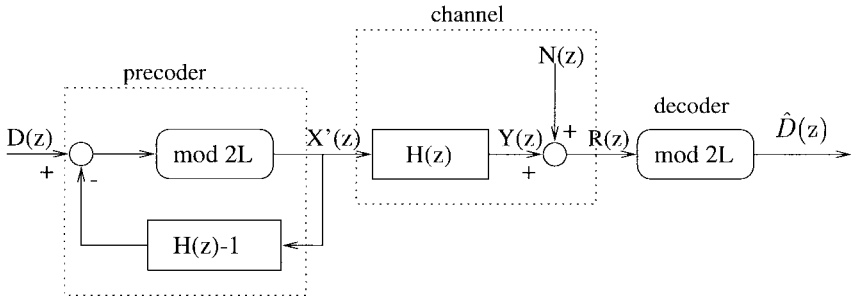

Fig. 2. Tomlinson–Harashima precoding system.

for some complex integer k_i such that $|\mathrm{Re}(x_i')| < L$ and $|\mathrm{Im}(x_i')| < L$. The corresponding z transform of the transmitted sequence $\{x_i'\}$ is

$$X'(z) = D(z) + 2LK(z) - X'(z)[H(z) - 1]$$
$$\Rightarrow X'(z) = \frac{[D(z) + 2LK(z)]}{H(z)} \tag{6}$$

where $D(z)$ and $K(z)$ are the z transform of the sequence $\{d_i\}$ and $\{k_i\}$, respectively. The received sequence $\{r_i\}$ in a noise-free situation has the following z transform:

$$R(z) = X'(z)H(z) = D(z) + 2LK(z) \tag{7}$$

which corresponds to $r_i = d_i + 2Lk_i$. The desired signal d_i is recovered at the receiver by applying the same modulo operation to the received signal. Since $|\mathrm{Re}(d_i)| < L$ and $|\mathrm{Im}(d_i)| < L$, $[r_i \bmod 2L]$ must give d_i.

In this paper, we view the operation of the TH precoding in light of dimension partitioning as follows. The $L \times L$ QAM can be represented by its square signal constellation (centered at the origin with side length equal to $2L$) defined on a two-dimensional (2-D) Euclidean space. The desired signal d_i, which is also the input signal of the precoder, can be represented by the corresponding point in the constellation. Because of the feedback path in the precoder, the input signal applied to the modulo-$2L$ operator of the precoder is defined on the whole Euclidean space. Hence, the 2-D Euclidean space is referred to as the signal space. The TH precoder has three functions.

1) *Dimension Partitioning*: The modulo-$2L$ operator partitions the signal space into nonoverlapping square regions of side $2L$. Each of such regions is referred to as a partition. The partition centered at the origin is referred to as the base partition, over which the QAM signal constellation is defined. All other partitions can be viewed as a replica of the base partition except that the centers of the partitions are shifted correspondingly. In other words, the desired signal d_i has a corresponding constellation point in each partition. The dimension partitioning corresponding to TH precoding is referred to as TH partitioning.
2) *Selecting a Shifted Desired Constellation Point*: Based on the ISI component I_i represented by a point in the signal space (called the ISI point), the precoder chooses the replica of the desired signal constellation point in such a partition that the selected point is closest to I_i. The selected point, referred to as the shifted desired constellation point, represents the desired signal after the modulo-$2L$ operation.
3) *Precoding the Transmitted Signal*: The precoder calculates the difference between the shifted desired constellation point and the ISI point and sends the difference as the precoded signal.

After the precoded signal travels along the frequency-selective fading channel, the received signal is represented by the shifted desired constellation point in the signal space in the absence of additive white Gaussian noise. The decoder at the receiver (which is a modulo-$2L$ operator) moves the shifted desired constellation point back to the base partition and gives the desired signal as the output. An example of TH precoding is shown in Fig. 3, where the desired signal d_i is represented by the constellation point • in the base partition, and the replica of the constellation point in all other partitions is also shown.

In the above discussion, $h_0 = 1$ is assumed. However, when the first-path signal experiences fading, the assumption is no longer true. To compensate the effect, the estimated channel response is normalized with respect to h_0 before applying to the precoder. The precoded signal is then multiplied by $1/h_0$ before transmission in order to counteract the first-path fading effect on the received signal. As a result, the receiver can recover the signal without knowing the value of h_0. TH precoding was originally proposed for a wired communication system which does not have the problem of channel fading. When directly applied to a wireless communication system, TH precoding suffers the following three drawbacks.

1) To cancel ISI, TH precoding results in a variable transmitted signal amplitude. When PSK is used, TH precoding may not be a desirable technique. Using PSK, a constant transmitted signal amplitude is desired as explained earlier. If one tries to confine TH precoding with a constant transmitted signal amplitude, it may be impossible to define a precoded signal which results in the received signal lying within the correct decision region. Fig. 4 shows a possible situation where TH precoding with constant signal amplitude A does not work for sending the desired signal. With a constant transmitted amplitude A and $h_0 = 1$, the received ISI-free signal can only lie on a circle centered at the ISI with radius equal to A. This circle is called ISI circle. The ISI circle does not overlap with the correct decision region for the signal, thus, no precoded signal

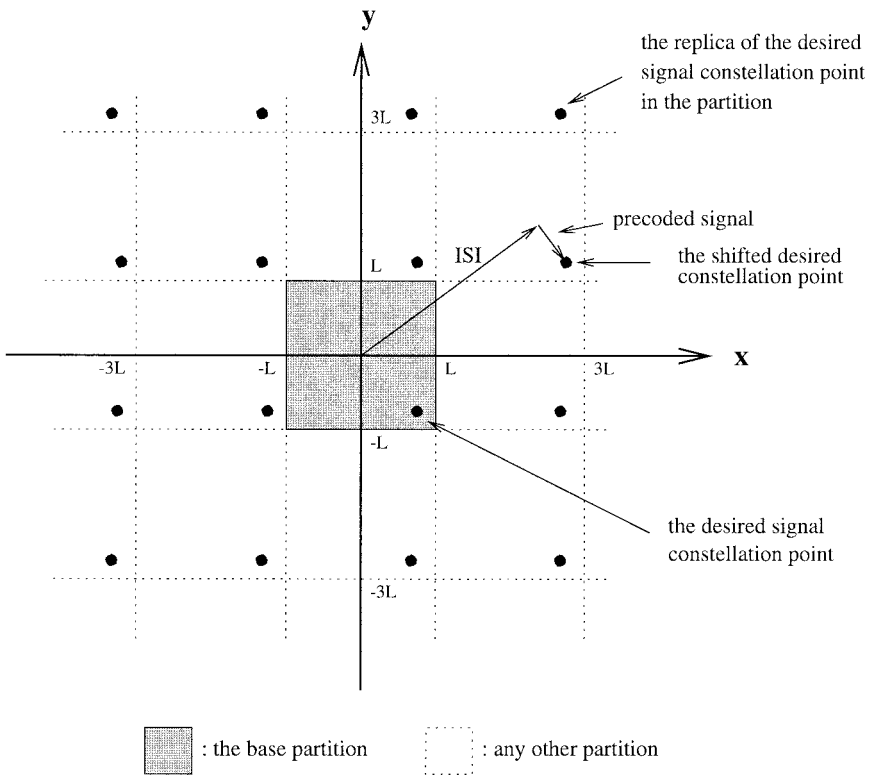

Fig. 3. Dimension partitioning in TH precoding.

with constant amplitude A is likely to give a correctly detected data at the receiver.

2) The TH precoded signal is vulnerable to additive noise introduced by the channel, due to the fact that TH partitioning reduces decision regions for signal constellation points. A small noise component can shift the received signal from the correct decision region to an incorrect decision region and result in transmission error, as illustrated in Fig. 5.
3) In a wireless system, deep fading on the first path is very common. When it happens, the compensation factor $1/h_0$ by which the signal is multiplied before transmission may become impractically large. In the extreme case when h_0 tends to zero, the precoder will become unstable.

In the following, we develop a new precoding technique for the indoor wireless system, which can overcome the drawbacks of TH precoding.

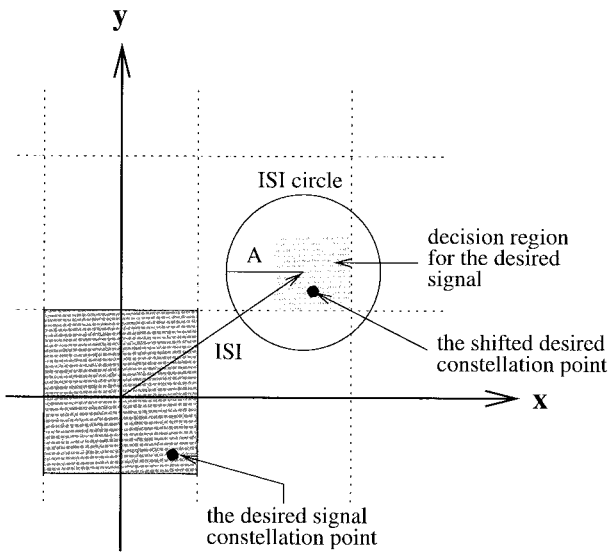

Fig. 4. Drawback of TH precoding for constant amplitude modulation.

B. The New Dimension Partitioning

The second drawback of the TH precoding results from the TH partitioning which greatly reduces the signal decision region for each signal constellation point. As a result, transmission BER due to AWGN is significantly increased. The problem can be mitigated to a certain degree if the adjacent regions in the adjacent partitions represent the same data symbol. This can be achieved by flipping the partitions (from TH partitioning) in such a way that regions representing the same data symbol in QPSK stick together to form a larger decision region. This results in the dimension partitioning of the signal space shown in Fig. 6, which is referred to as flipped partitioning. As a result, small perturbations of the received signal due to noise can move the signal point only to another region representing the same data symbol in the adjacent partitions and result in no detection error. However, even with the flipped partitioning, there is still the problem of constraining the transmitted signal amplitude to a constant (i.e., the first drawback of the TH partitioning remains). It is possible that the precoded signal can result in a transmission error even under a noise-free condition because the received

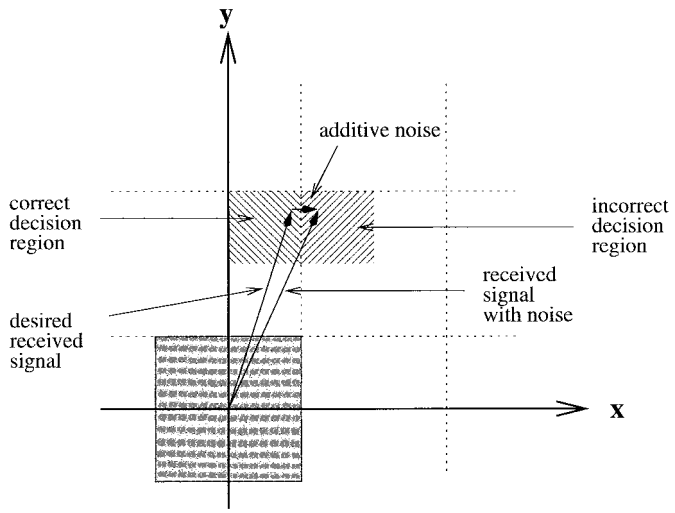

Fig. 5. Signal shift due to noise in TH precoding.

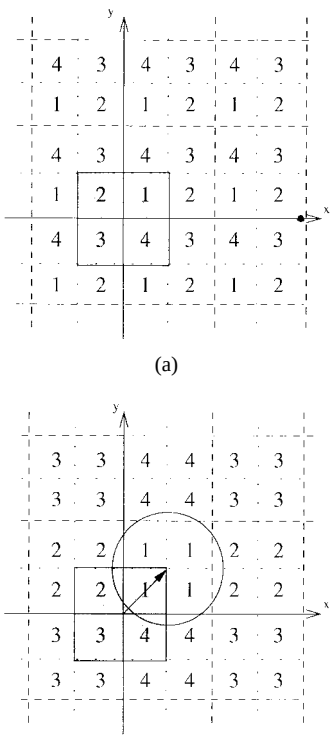

(a)

(b)

Fig. 6. TH partitioning and flipped partitioning ("1"= $\pi/4$, "2" = $3\pi/4$, "3" = $5\pi/4$, and "4" = $7\pi/4$).

signal can only lie on the ISI circle when the transmitted amplitude is constant. Fig. 6 shows a possible situation that the ISI circle does not overlap with any of the decision regions representing the QPSK signal of phase $5\pi/4$. Hence, the data represented by the phase $5\pi/4$ cannot be correctly detected. To overcome the first drawback of the TH partitioning, we have to further modify the flipped partitioning.

The objective of channel equalization or channel precoding is to increase the probability of correct detection. To achieve this objective, TH precoding tries to completely remove ISI. In the absence of noise, the TH decoder output at the receiver

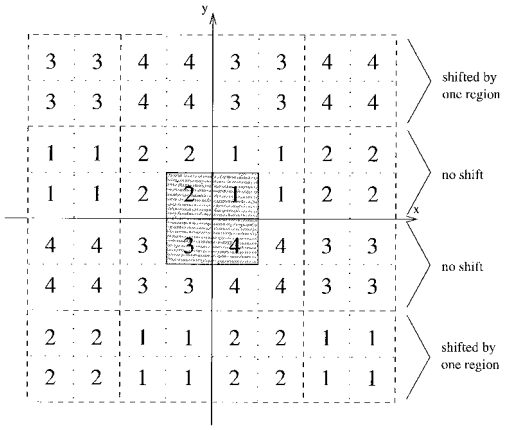

Fig. 7. The new dimension partition.

is exactly the same as the TH precoder input at the transmitter. However, this is not necessary for correct detection. As long as the signal applied to the decision device lies in the correct decision region, there will be no transmission error. For example, if we intend to send a 2-b symbol "00" represented by the QPSK signal of phase $\pi/4$, the decoder output signal can have a phase anywhere between 0 to $\pi/2$ in order to allow the decision device to make a correct decision. As a result, a precoding scheme can reduce the BER as long as the precoder can find a signal point in the appropriate region all the time (even if the decoded signal is not exactly the same as that before precoding). From this point of view, we shift one row of the flipped partitions in every two rows to the left by one partition, resulting in the final partitioning shown in Fig. 7. With this new dimension partitioning, the ISI circle always overlaps with all the regions representing the four different phases of QPSK signal if the constant amplitude A of the precoded signal is within the range of $[5L/4, \sqrt{2}L]$.

C. Precoding and Decoding Procedures

To precode a signal, we first estimate the ISI from the known channel information and the previously transmitted signals. Using this estimated ISI (the ISI point) as the center, the ISI circle can be drawn. The best signal point on the ISI circle is found on the partitioned 2-D signal space and the difference between the ISI point and this best signal point will be sent as the precoded signal. "The best signal point" means the point which will result in the least probability of error. However, to find this point may need complex mathematical calculation. For example, for a fading channel with AWGN, it involves calculations of complex Q function. Fortunately, because the probability of error of a 2-D signal is usually dominated by one of the in-phase and quadrature noise components, we can simplify the calculation process. Define the worst case noise margin of a signal point as the smaller component of the noise margin in the in-phase or quadrature direction, and the signal point with the largest worst case noise margin can be used as the best signal point.

Operationally, the estimated ISI is first truncated through the modulo-arithmetic operation such that both the in-phase and quadrature components of the truncated ISI are in the range

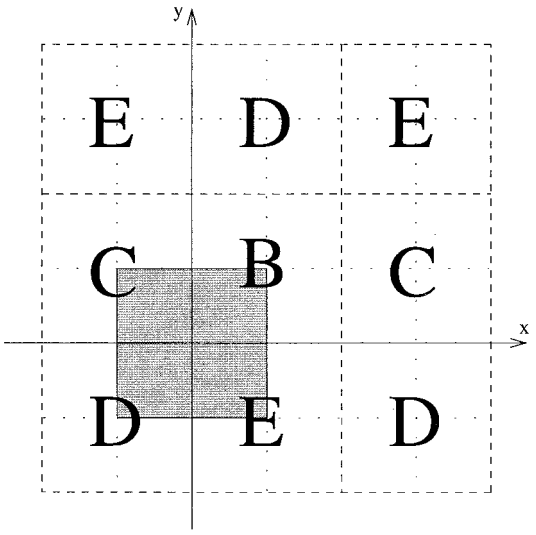

$(m_i \bmod 2, n_i \bmod 4), B, C, D, E$
$(0,0) or (1,2), \pi/4, 3\pi/4, 5\pi/4, 7\pi/4$
$(0,1) or (1,3), 7\pi/4, 5\pi/4, \pi/4, 3\pi/4$
$(0,2) or (1,0), 3\pi/4, \pi/4, 7\pi/4, 5\pi/4$
$(0,3) or (1,1), 7\pi/4, 5\pi/4, \pi/4, 3\pi/4$

Fig. 8. Relationship between (m_i, n_i) and partition pattern.

$[0, 2L]$. The truncation is performed by adding $2(m_i + jn_i)L$ (for some integers m_i and n_i) to the estimated ISI. In the original TH precoding, no matter what values m_i and n_i are, the modulo operations do not change the phase (or symbol) represented by each of the four regions in any partition, as shown in Fig. 6. However, due to the partition flipping and shifting in the new dimension partitioning, different combinations of m_i and n_i result in that the same (enlarged) region represents different phases. Fig. 8 shows the relations between (m_i, n_i) and the phase represented by each region after the modulo operations. Depending on what the combination is, each region of B, C, D, and E in Fig. 8 corresponds to a particular phase. Note that the truncated ISI always lies in region B. In the following, we generally consider cases of desirable phase represented by each of the B, C, D, and E regions instead of the actual phase such as $\pi/4, 3\pi/4$, etc. The Appendix gives the details of how to calculate the best signal point according to which region (B, C, D, or E in Fig. 8) represents the information symbol to be transmitted.

In summary, the precoding procedure is as follows.

Step 1: Calculate the estimated ISI according to the channel information and the previously transmitted symbols.

Step 2: Represent the estimated ISI by the truncated ISI and the numbers (m_i and n_i) of the modulo-arithmetic operations performed.

Step 3: Determine which region (B, C, D, or E) represents the information symbol to be transmitted according to Fig. 8 and the values of m_i and n_i.

Step 4: Find the best signal point based on the truncated ISI and the region representing the information symbol (as given in the Appendix).

Step 5: Send the difference between the truncated ISI and the best signal point as the precoded signal.

The transmitted signal is corrupted by the dispersive fading channel and AWGN. To recover the transmitted information symbol, the decoder at the receiver applies the same modulo-arithmetic operation on the received signal and keeps track of the numbers of modulo operations. With the received signal over the ith symbol interval r_i, the signal after modulo operations is

$$\hat{d}_i = r_i - 2(\hat{m}_i + j\hat{n}_i)L \tag{8}$$

for some integer $\hat{m}_i$ and $\hat{n}_i$ such that $|\mathrm{Re}(\hat{d}_i)| < L$ and $|\mathrm{Im}(\hat{d}_i)| < L$. The values of $\hat{m}_i$ and $\hat{n}_i$ are applied to the decision device together with the truncated received signal $\hat{d}_i$. The decision device uses $\hat{m}_i$ and $\hat{n}_i$ to define the meanings of the decision regions according to Fig. 8 and then makes the decision based on the truncated received signal $\hat{d}_i$.

D. First-Path Fading Estimation

In the above development of the new precoding technique, it is assumed that $h_0 = 1$. To overcome the third drawback of the TH partitioning, the first-path fading must be taken into consideration for indoor wireless applications. From the estimated channel information in the reverse link, the estimated ISI should be normalized with respect to h_0 $(= \alpha_0 e^{j\phi_0})$ in the precoding procedure so that the equivalent channel gain in the first path is still unity. Before being transmitted, the precoded signal is multiplied by $e^{-j\phi_0}$ such that the phase distortion ϕ_0 due to the channel is eliminated. No amplitude compensation for α_0 is performed to the precoded signal.

The first-path amplitude fading is taken into account at the receiver. Since the transmitter has normalized the estimated ISI, the decoder at the receiver should use the scaled side length $2\alpha_0 L$ of the decision region and transmitted amplitude $\alpha_0 A$. Therefore, the receiver needs to know the amplitude fading α_0. In a slowly fading channel, the fading of the first path remains approximately unchanged over a data frame and the receiver can use a training sequence to estimate this attenuation. In general, the training sequence contains two types of symbols, with a phase shift of 180° between them. A variable can be formed in such a way that the signal components from all delayed paths cancel each other and the remaining component comes only from the first path. For example, we can send $\{1,1,0,1,0,0,1,1,1\}$ as a training sequence for a channel with three delayed paths [i.e., $K = 3$ in (2)], where symbol zero represents $Ae^{j\pi/4}$ and one represents $Ae^{j5\pi/4}$. With r_i being the ith received complex signal, we can form the components of $r_4 + r_8, -(r_5 + r_6), r_7 + r_9$, all of which follow Gaussian distribution with mean $2A\alpha_0$ and variance $4\delta_N^2$ which is twice the power of the complex received noise at baseband. The variable, which is defined as

$$\hat{\alpha}_0 = \left| \frac{r_4 - r_5 - r_6 + r_7 + r_8 + r_9}{6} \right| \tag{9}$$

follows a Gaussian distribution with mean $A\alpha_0$ and variance $\delta_N^2/3$. We can use the variable as an estimator of the amplitude fading of the first path. The decoder uses $2\hat{\alpha}_0 L$ to perform the

modulo-arithmetic operation. The accuracy of the estimation is better if a longer training sequence is used or if there exists fewer multiple paths. For a channel with K delayed paths, if a training sequence of $2n + K$ symbols is used, an estimator $\hat{\alpha}_0$ following a Gaussian distribution with mean $A\alpha_0$ and variance δ_N^2/n can be obtained. This overhead is justified when compared with that using a DFE, since a training sequence of length larger than twice the number of taps is necessary when the recursive least squares (RLS) algorithm is used to update the tap coefficients of the DFE [18]. With the estimation of α_0, the first-path fading is compensated at the receiver instead of the transmitter. As a result, precoder stability can be achieved and the transmitted signal amplitude can be kept constant even when the first path experiences deep fading.

E. Discussion

So far, we have described the new precoding scheme with a constant transmitted signal amplitude for QPSK. Four issues concerning the precoding scheme need to be addressed.

1) In the above discussion, the first-path signal is considered to be the desired signal, and only postcursors are considered in precoding. In general, the desired path should be the one which has a larger average power than that of any other paths. Usually, the desired path is the first path in an indoor radio environment [14]. In the case where the first path does not have the maximum average power, channel equalization should combat precursors in the channel impulse response in order to achieve optimum transmission performance. In the DFE at the base-station receiver, the effect of precursors is mitigated by a linear feedforward filter, and the postcursors (tails) are removed by a feedback filter with previously detected decisions as input. Similarly, if precursors should be considered in the precoding scheme, a linear feedforward filter can be used with the same tap number and tap gain coefficients, respectively, as those of the feedforward filter in the DFE [19]. The filter can be inserted either after the precoder at the transmitter or before the signal detector at the receiver. Since inserting the filter in the transmitter would result in nonconstant transmitted signal amplitude, it is preferred that the filter be inserted at the receiver front end. There are two ways for the receiver to determine the tap coefficients of the filter: a) the base station transmits the information to the receiver, which achieves the receiver simplicity at the expense of transmission overhead and b) the receiver linearly equalizes the precursors by continuously adapting the coefficients to maintain the overall channel response that the precoder expects [19], [20]. Although using the linear feedforward filter at the receiver increases the complexity of the portable units, the complexity does not increase when the coded modulation and Viterbi decoder are used because no decision feedback is required by the linear equalizer. The complexity of a portable unit using the linear equalizer with a precoder at the base station is significantly reduced as compared with that using a DFE because the DFE requires zero-delay decision feedback.
2) In the decoding process, the algorithm is proposed for the receiver to estimate the first-path amplitude fading, which uses a straightforward sample average as given in (9). The receiver then uses the estimated amplitude in the modulo-arithmetic operation. It will be shown in Section V that the accuracy of the estimation affects the performance of the precoding method even though the effect is not significant. Because the effect of the first-path estimation error is severe only when the channel undergoes deep fading, the transmission performance can be further improved by combining the precoding with other channel impairment mitigation techniques, such as diversity, to reduce the effect of deep fading.
3) In a conventional communication system, DFE has generally been preferred to precoding, since it does not require the channel information at the transmitter. Compared with a DFE, the advantages of channel precoding lie in that: a) no decision feedback is necessary at the portable unit receiver which can greatly reduce the complexity of the portable unit when coded modulation is used and b) there is no error propagation, which can improve the system transmission performance. These are the motivation for precoding before the channel for a low-power indoor wireless communication system, where the channel is characterized by frequency-selective slowly fading and the simplicity of the portable units is desirable.
4) Although only the application of the proposed precoding method to the conventional QPSK has been studied in this paper, extensions to other QPSK modulation is straightforward. For example, when the precoding method is applied to differential $\pi/4$-shifted QPSK (the modulation scheme used in the North American Digital Cellular System, IS-54 Standard [21]), the only modification needed is to use different modulo operation parameters for the odd and even symbols, respectively. The possibility of applying this precoding method to MPSK modulation $(M > 4)$ is yet to be explored. Since partition flipping and shifting depend on the shape of the decision region, MPSK with different decision region shapes needs different treatment. It would be useful to extend the precoding method to higher order MPSK so that the system performance can be further improved by combining the precoding with trellis-coded modulation (TCM) [22]. With QPSK, only rate 1/2 TCM can be used. With high-order TCM using MPSK, additional transmitted power can be saved in achieving the same BER performance.

IV. Theoretical Transmission Performance Analysis

Performance analysis of the newly proposed precoding technique with absolute phase-encoded QPSK is considered in this section. The following assumptions are made: 1) the precoder has channel information such that the estimated ISI is accurate; 2) at the receiver, the carrier phase is recovered

perfectly and the first-path amplitude fading is estimated accurately; and 3) the channel is assumed to be two-path time variant with the propagation delay difference between the two paths equal to one symbol interval T. The first path experiences Rician fading or Rayleigh fading, and the second path experiences Rayleigh fading. It should be noted that this model presents a rough approximation of a practical frequency-selective fading channel [21]. For a slowly fading channel, the amplitude fluctuations $\alpha_0(t)$ and $\alpha_1(t)$ and phase jitters $\phi_0(t)$ and $\phi_1(t)$ are approximately time invariant over one symbol interval. The ith received symbol at baseband is

$$r_i = A[\alpha_0 e^{j(\phi_0+\theta_i)} + \alpha_1 e^{j(\phi_1+\theta_{i-1})}] + N_i \tag{10}$$

where $\alpha_0 = \alpha_0(iT)$, $\alpha_1 = \alpha_1(iT)$, $\phi_0 = \phi_0(iT)$, $\phi_1 = \phi_1(iT)$, and N_i is the complex received AWGN noise at baseband with zero mean and variance $2\delta_N^2$. Without losing generality, we use $A = 1$ and the ISI is $\alpha_1 e^{j(\phi_1+\theta_{i-1})}$. Since ϕ_1 is uniformly distributed over $[0, 2\pi]$ by assumption 3), the combined phase $(\phi_1+\theta_{i-1})$ is also uniformly distributed over $[0, 2\pi]$. Combined with the Rayleigh distributed α_1, the ISI can be split into in-phase and quadrature components which are independent and Gaussian distributed with zero mean and variance δ_2^2 when the average power carried by the second path is $2\delta_2^2$. After modulo-arithmetic operation and normalizing the ISI with respect to the amplitude fading α_0 of the first path, the conditional probability density functions (pdf's) for the in-phase (X) and quadrature (Y) components of the truncated ISI are

$$f_{X|\alpha_0}(x_I) = \frac{\alpha_0}{\sqrt{2\pi}\delta_2} \sum_{i=-\infty}^{\infty} \exp\left[-\frac{\alpha_0^2(2iL+x_I)^2}{2\delta_2^2}\right], \quad x_I \in [0, 2L) \tag{11}$$

$$f_{Y|\alpha_0}(y_I) = \frac{\alpha_0}{\sqrt{2\pi}\delta_2} \sum_{i=-\infty}^{\infty} \exp\left[-\frac{\alpha_0^2(2iL+y_I)^2}{2\delta_2^2}\right], \quad y_I \in [0, 2L) \tag{12}$$

respectively. Note that $f_{X|\alpha_0}(x_I)$ is symmetric about $x_I = L$ and $f_{Y|\alpha_0}(y)$ about $y_I = L$.

With the truncated ISI, the probability that a received signal lies outside the desired decision region for a given best signal point (x, y) (where $x \in [0, 2L]$ and $y \in [0, 2L]$) is, as shown in Fig. 9

$$\begin{aligned} Q_1(x,y) = {} & Q\left(\frac{\alpha_0}{\delta_N}x\right) + Q\left(\frac{\alpha_0}{\delta_N}(2L-x)\right) + Q\left(\frac{\alpha_0}{\delta_N}y\right) \\ & + Q\left(\frac{\alpha_0}{\delta_N}(2L-y)\right) - Q\left(\frac{\alpha_0}{\delta_N}x\right)Q\left(\frac{\alpha_0}{\delta_N}y\right) \\ & - Q\left(\frac{\alpha_0}{\delta_N}x\right)Q\left(\frac{\alpha_0}{\delta_N}(2L-y)\right) \\ & - Q\left(\frac{\alpha_0}{\delta_N}(2L-x)\right)Q\left(\frac{\alpha_0}{\delta_N}y\right) \\ & - Q\left(\frac{\alpha_0}{\delta_N}(2L-x)\right)Q\left(\frac{\alpha_0}{\delta_N}(2L-y)\right) \end{aligned} \tag{13}$$

where

$$Q(x) = \frac{1}{\sqrt{2\pi}} \int_x^{\infty} \exp\left(-\frac{t^2}{2}\right) dt.$$

When the data is represented by region B (Case 1) or C (Case 2), the precoding procedures are symmetric about $x = L$ and $y = L$. Therefore, we consider only the situation that the truncated ISI is in the lower left quarter of region B. In Case 1, if we define

$$h(x,y) = \frac{x+y+\sqrt{2-(x-y)^2}}{2} \tag{14}$$

then from the coordinates of the best signal point, given by (29) in the Appendix, the conditional probability of symbol error given α_0 is

$$\begin{aligned} P_{e|1,a_0} = {} & 4\int_0^L \int_0^L Q_1(h(x_I,y_I), h(x_I,y_I)) f_{X|\alpha_0}(x_I) \\ & \cdot f_{Y|\alpha_0}(y_I)\, dy_I\, dx_I. \end{aligned} \tag{15}$$

In Case 2, the coordinates of the best signal point are given by (36) and (37) in the Appendix. If we define

$$l(x,y) = \frac{x-y-\sqrt{2-(x+y)^2}}{2} \tag{16}$$

then the conditional probability of symbol error is

$$\begin{aligned} P_{e|2,\alpha_0} = {} & 4\int_0^{1-L} \int_0^L Q_1(-l(x_I,y_I), -l(x_I,y_I)) \\ & \cdot f_{X|\alpha_0}(x_I) f_{Y|\alpha_0}(y_I)\, dy_I\, dx_I \\ & + 4\int_{1-L}^L \int_0^{1-x_I} Q_1(-l(x_I,y_I), -l(x_I,y_I)) \\ & \cdot f_{X|\alpha_0}(x_I) f_{Y|\alpha_0}(y_I)\, dy_I\, dx_I \\ & + 4\int_{1-L}^L \int_{1-x_I}^L Q_1(1-x_I, y_I) f_{X|\alpha_0}(x_I) \\ & \cdot f_{Y|\alpha_0}(y_I)\, dy_I\, dx_I. \end{aligned} \tag{17}$$

In (17), we have made use of the fact that, for a given best signal point (x, y) with $-2L \le x \le 0$ and $0 \le y \le 2L$, we can still use the function $Q_1(\cdot)$ defined in (13) to represent the probability that the received signal lies outside the desired decision region by shifting the coordinates into the region $x \in [0, 2L]$ and $y \in [0, 2L]$. Therefore, we replace (x, y) by $(x + 2L, y)$ in $Q_1(\cdot)$. Furthermore, since $Q_1(x, y) = Q_1(2L - x, y)$, $Q_1(x + 2L, y)$ can be written as $Q_1(-x, y)$. Combined with (16), the result in (17) is obtained.

In the case that the data is represented by region D (Case 3), the precoding procedure is symmetric about $x = L$. We need to consider only the situation that the truncated ISI lies in the left half of region B. If we define

$$m(x,y) = \frac{x+y-2L+\sqrt{2-(x-y+2L)^2}}{2} \tag{18}$$

$$n(x,y) = \frac{x+y-\sqrt{2-(x-y)^2}}{2} \tag{19}$$

then from the coordinates of the best signal point [(42), (43), and (45) in the Appendix], the conditional probability of symbol error is

$$\begin{aligned} P_{e|3,a_0} = {} & 2\int_0^{x_0} \int_{s(x_I)}^{2L} Q_1(m(x_I,y_I), m(x_I,y_I)) \\ & \cdot f_{X|\alpha_0}(x_I) f_{Y|\alpha_0}(y_I)\, dy_I\, dx_I \end{aligned}$$

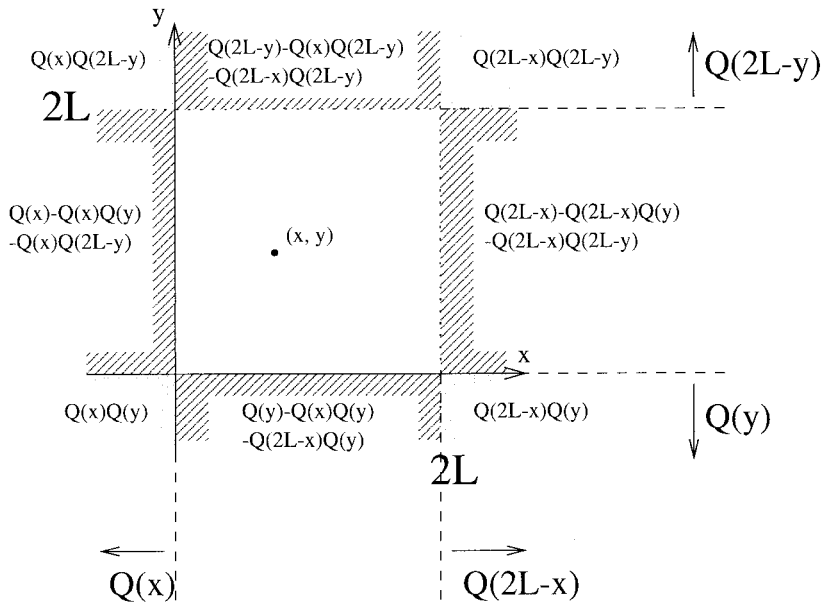

Fig. 9. Probability of symbol error given the best signal point coordinates (x, y).

$$
\begin{aligned}
&+2\int_{x_0}^{L}\int_{2L-1+x_I}^{2L} Q_1(m(x_I,y_I),m(x_I,y_I))\\
&\cdot f_{X|\alpha_0}(x_I)f_{Y|\alpha_0}(y_I)\,dy_I\,dx_I\\
&+2\int_{0}^{x_0}\int_{0}^{s(x_I)} Q_1(-n(x_I,y_I),-n(x_I,y_I))\\
&\cdot f_{X|\alpha_0}(x_I)f_{Y|\alpha_0}(y_I)\,dy_I\,dx_I\\
&+2\int_{x_0}^{L}\int_{0}^{r(x_I)} Q_1(-n(x_I,y_I),-n(x_I,y_I))\\
&\cdot f_{X|\alpha_0}(x_I)f_{Y|\alpha_0}(y_I)\,dy_I\,dx_I\\
&+2\int_{x_0}^{L}\int_{r(x_I)}^{2L-1+x_I} Q_1(x_I,1-2L+y_I)\\
&\cdot f_{X|\alpha_0}(x_I)f_{Y|\alpha_0}(y_I)\,dy_I\,dx_I
\end{aligned}
\tag{20}
$$

where $r(x_I)$ and $s(x_I)$ are the y_I coordinate for a given x_I coordinate defined by (44) and (46), respectively, in the Appendix. $r(x_I)$ can be written as (21), given at the bottom of the page. In order to simplify the calculation, $s(x_I)$ can be approximated by

$$s(x_I)=\left(\frac{y_0-L}{x_0}\right)x_I+L \tag{22}$$

where x_0 and y_0 are given by (47) in the Appendix. When the data is represented by region E (Case 4), the conditional probability of symbol error can also be calculated by (20) since the precoding procedure in Case 4 is the mirror image of that in Case 3 about $y=L$.

If the message symbols ("00," "01," "10," and "11") are equiprobable, the four cases are equiprobable. The overall probability of symbol error is

$$P_e=\int_0^{\infty}\tfrac{1}{4}\left[P_{e|1,\alpha_0}+P_{e|2,\alpha_0}+2P_{e|3,\alpha_0}\right]f_R(\alpha_0)\,d\alpha_0 \tag{23}$$

where $f_R(\cdot)$ is the Rician or Rayleigh distribution, depending on the characteristics of the first-path fading under consideration.

To calculate the BER, we have to modify the $Q_1(\cdot)$ function defined in (13). It should be noted that, out of the four possibilities of the recovered data, one of them corresponds to the correct data, two to a 1-b error and only one to a 2-b error. In Fig. 8, with the coordinates of the best signal point being (x,y), if the transmitted data is represented by region B, then a received signal that lies in C regions will cause a 1-b error out of the two transmitted bits and the probability of this occurrence is

$$
\begin{aligned}
Q_C(x,y)=&\,Q\left(\frac{\alpha_0}{\delta_N}x\right)+Q\left(\frac{\alpha_0}{\delta_N}(2L-x)\right)\\
&-Q\left(\frac{\alpha_0}{\delta_N}x\right)Q\left(\frac{\alpha_0}{\delta_N}y\right)-Q\left(\frac{\alpha_0}{\delta_N}x\right)\\
&\cdot Q\left(\frac{\alpha_0}{\delta_N}(2L-y)\right)-Q\left(\frac{\alpha_0}{\delta_N}(2L-x)\right)\\
&\cdot Q\left(\frac{\alpha_0}{\delta_N}y\right)-Q\left(\frac{\alpha_0}{\delta_N}(2L-x)\right)\\
&\cdot Q\left(\frac{\alpha_0}{\delta_N}(2L-y)\right).
\end{aligned}
\tag{24}
$$

Furthermore, one of the D and E regions represents a 1-b error, and the other represents a 2-b error. Since the phase of the truncated ISI is uniformly distributed and the D and E

$$r(x_I)=\frac{-[6(1-2L)+2x_I]+\sqrt{-16x_I^2-16(1-2L)x_I-4(1-2L)^2+20}}{10} \tag{21}$$

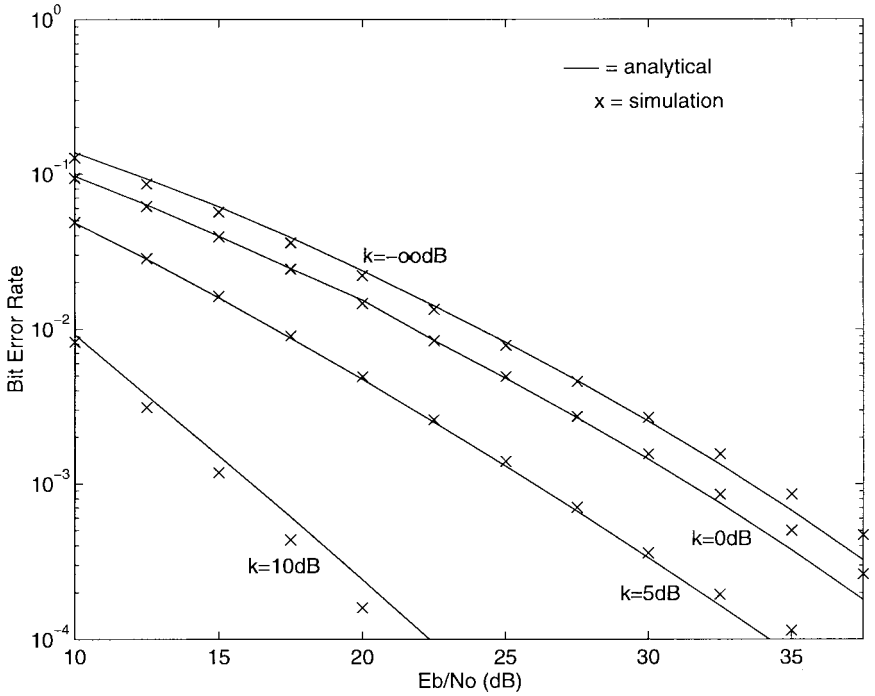

Fig. 10. BER for absolute phase-encoded QPSK using the precoder.

regions are symmetric, both D and E regions have the same probability of representing a 2-b error. Thus, on the average, a received signal that lies in D or E regions causes 1.5-b errors out of the two transmitted bits and the probability is

$$Q_{D,E}(x,y) = Q\left(\frac{\alpha_0}{\delta_N}y\right) + Q\left(\frac{\alpha_0}{\delta_N}(2L-y)\right). \tag{25}$$

As a result, the conditional probability of bit error, given the best signal point (x,y), is

$$Q_2(x,y) = 0.5Q_C(x,y) + 0.75Q_{D,E}(x,y) \tag{26}$$

and the overall BER can be calculated according to (23) except replacing $Q_1(\cdot)$ by $Q_2(\cdot)$ in (15), (17), and (20).

V. Numerical Results and Discussion

In order to verify the theoretical analysis, the performance of the newly proposed precoding method with absolute phase-encoded QPSK is investigated through computer simulation. In addition, the system using differentially encoded QPSK is also studied based on computer simulation. In the simulation, the same assumptions as those in the theoretical performance analysis of Section IV are made. The value of E_b/N_0 is the ratio of the ensemble average of the received signal power per bit from both paths to the variance $2\delta_N^2$ of the input Gaussian noise at baseband. The k-factor is defined as the ratio of the average power carried by the LOS component to that carried by the diffused component of the first path in a Rician fading channel. The values of k-factor under consideration are $-\infty$ dB (which corresponds to Rayleigh fading), 0, 5, and 10 dB. The average power carried by the diffused component of the second path is assumed to be the same as that of the first path.

A. Absolute Phase-Encoded QPSK

Fig. 10 shows the BER of the forward link when the precoding technique is used for absolute phase-encoded QPSK. Both numerical analysis results (based on the derivations in Section IV) and the corresponding simulation results are given. It is observed that: 1) the simulation results closely match with the analytical ones; 2) when the k-factor increases from 5 to 10 dB, the transmission performance is significantly improved. This is because, with a large value of the k-factor, the first path experiences much less deep fading when the k-factor value increases and the scaling effect of the first-path fading is relatively small. As a result, most of the time, $\alpha_0 L$ is large and the effect of noise is relatively small; 3) when the k-factor increases from $-\infty$ to 0 dB, the performance is only slightly improved. This is because the first path still undergoes deep fading frequently even when the k-factor value increases, and $\alpha_0 L$ can be very small. The effect of noise is relatively strong and thus results in a relatively large error rate; and 4) within the range of E_b/N_0 under consideration, there is no apparent error floor, which means arbitrarily low symbol error rate can be achieved at the expense of signal power for any value of the k-factor.

B. Differentially Encoded QPSK

Fig. 11 shows the BER performance of the forward link when the proposed precoding method is used with differentially encoded QPSK. For comparison, the BER performance of the system using a DFE (obtained based on computer simulation) is also shown in the figure. The DFE consists of a three-tap feedforward filter and a two-tap feedback filter. The equalization and carrier phase synchronization are jointly performed by the DFE at baseband [23]. The phase

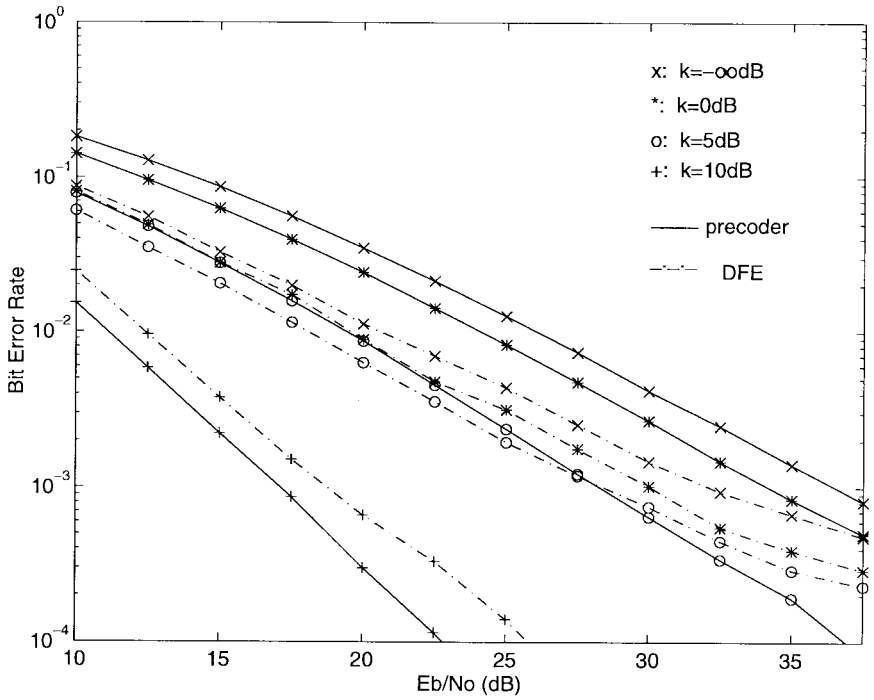

Fig. 11. BER for differentially encoded QPSK using the precoder and DFE with accurate channel information.

ambiguity in the joint optimization is avoided when using differentially encoded QPSK. Coherent detection and perfect symbol synchronization are assumed, as in the case of using the precoder. For a fair comparison between the precoder and DFE, it is assumed that accurate channel information is available for computing DFE tap coefficients. As a result, when the DFE is used with detected symbols fed back, the error propagation increases the BER value, but does not have any effect on the DFE tap coefficients which are set at their optimal values. It is observed that: 1) As the k-factor increases, the transmission performance using both precoder and DFE improves due to the fact that ISI component is reduced; 2) the DFE outperforms the precoder when the k-factor is small such as $-\infty$ to 0 dB because the proposed precoding technique reduces the size of decision regions due to dimension partitioning (especially when the first path experiences deep fading, i.e., the value of a_0 is very small) and because the constraint of constant signal amplitude may reduce the worst case noise margin depending on the value of the estimated ISI; 3) when the k-factor is increased to 5 dB, the precoder and DFE have almost the same performance. Under the channel condition, the effect of error propagation on degrading the DFE performance is comparable with the effect of the reduced decision regions on degrading the precoder performance; and 4) the precoder outperforms the DFE when the k-factor is further increased to 10 dB. With a strong LOS component (at the value of the k-factor), it is very unlikely for the first path to experience deep fading, therefore, the effect of the reduced decision regions on degrading BER performance is relatively small as compared with that of error propagation in the DFE. Since there is no decision feedback in the precoding process, errors in past decision do not affect the precoded signal and the detection of current symbol. As a result, there is no error propagation in the precoder. In general, DFE suffers from error propagation and the precoder suffers from the reduced decision regions. Whether or not the precoder has better performance depends on channel fading characteristics. When diversity reception is implemented to combat channel deep fading, it is very likely that the precoder can have better performance than a DFE.

C. Effect of the First-Path Fading Estimation

To study the effect of estimation accuracy of the first-path amplitude fading, simulation results are obtained based on the assumption that α_0 is estimated from a training sequence of 14 symbols. The estimated value $\hat{\alpha}_0$ has a Gaussian distribution with mean α_0 and variance $\delta_N^2/6$. Fig. 12 shows the BER simulation results when the estimated $\hat{\alpha}_0$ is used in the decoding at the receiver. By comparing Fig. 12 with Fig. 11, it is observed that the performance is degraded by the first-path estimation error. At a low E_b/N_0, the transmission error due to AWGN dominates and the effect of first-path estimation error is relatively small, therefore, the performance is only slightly degraded by the first-path estimation error. However, when the E_b/N_0 increases, the number of transmission errors due to AWGN decreases, and the effect of the first-path estimation error becomes dominant. At a small k-factor value, the ISI is severe and the number of modulo operations is large. Since the receiver uses $\hat{\alpha}_0 L$ in the modulo operation, the effect of the first-path estimation error is amplified by the large number of modulo operations. On the other hand, at a large k-factor value, the ISI is usually small and only a few or even no modulo operations are required to recover the signal. Thus, the first-path estimation error does not degrade the performance as much as in the case of a small k-factor value. In Fig. 13, the effect of different training sequence

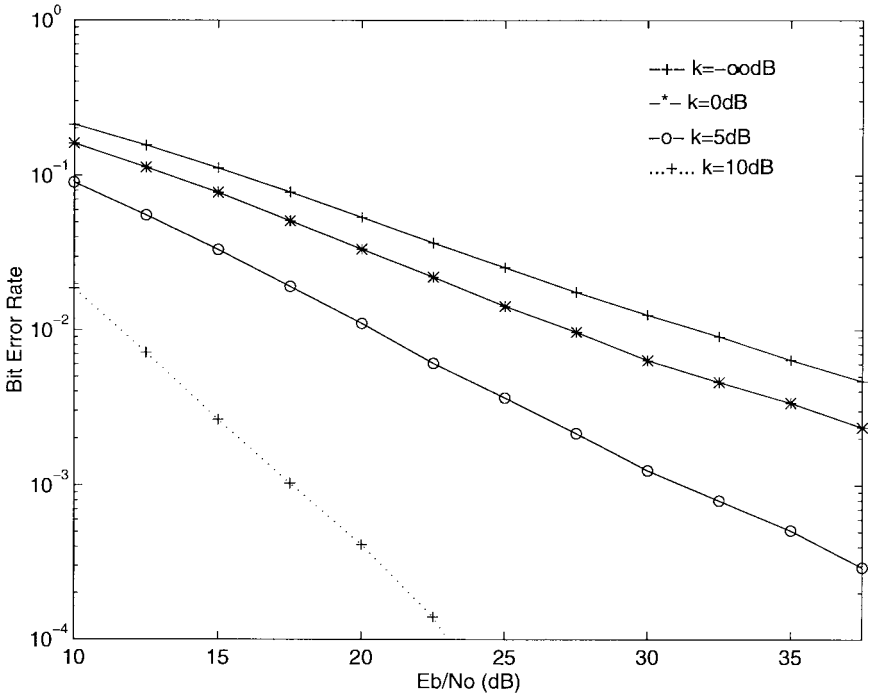

Fig. 12. BER for differentially encoded QPSK using the precoder with estimated $\hat{\alpha}_0$.

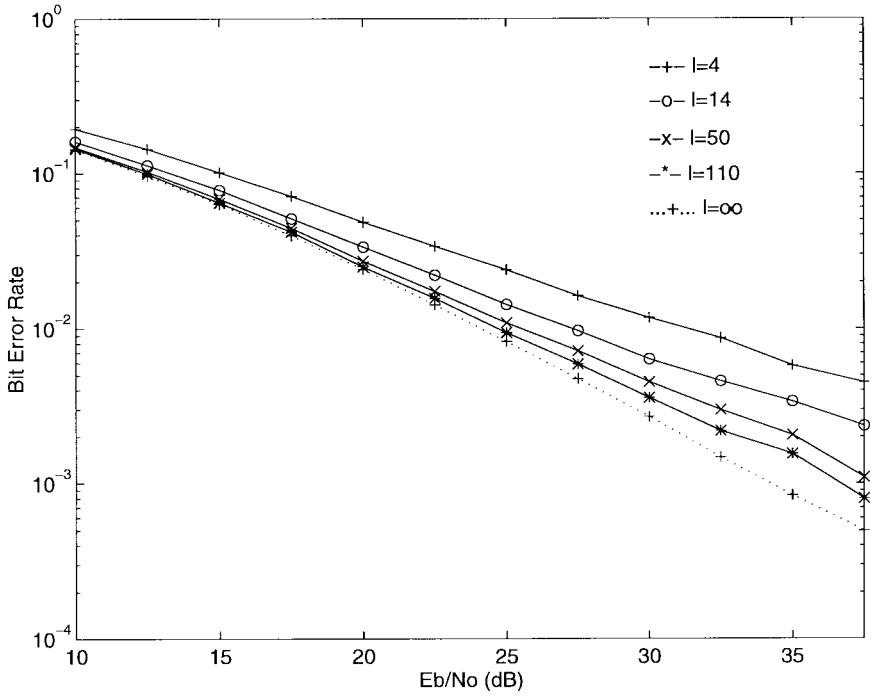

Fig. 13. BER for differentially encoded QPSK using the precoder with α_0 estimated from training sequences of different lengths ($k = 0$ dB).

length l is studied. As expected, the longer the training sequence, the more accurate the estimation and the better the BER performance. For $l = 110$, there is only a 2-dB difference from that using the exact α_0 at $E_b/N_0 = 35$ dB. However, such a long training sequence may not be practical. A training sequence of 14 symbols seems to be a reasonable choice.

VI. Conclusions

A new channel precoding technique with a constant transmitted signal amplitude has been developed for QPSK over frequency-selective slowly fading channels. Based on the new dimension partitioning, the precoder predistorts only the phase of the transmitted signal and keeps the transmitted signal amplitude constant. The precoding technique can be applied

to a high-rate TDMA/TDD indoor radio system, where ISI problem is a major concern and where the reciprocity of the radio links can be exploited. The channel information estimated in the reverse link can be used to precode the signal transmitted in the forward link in order to achieve ISI-free transmission. The advantages of the newly proposed precoding technique are that: 1) ISI-free transmission can be achieved without increasing the complexity of portable units; 2) the frequency spectrum in wireless communications can be utilized more efficiently as compared with that of the conventional 2×2 QAM using TH precoding; 3) the precoder is always stable; and 4) there is no error propagation problem. Theoretical analysis and computer simulation results have shown that the system using the proposed channel precoder can achieve a BER comparable with that using a conventional DFE. The precoder can outperform a DFE in an indoor environment where there is a strong LOS propagation path. The precoding method is especially useful for a low-power indoor wireless communication system, where the channel is characterized by frequency-selective slowly fading and where the simplicity of the portable units is desirable.

APPENDIX
COORDINATES OF THE BEST SIGNAL POINT

A. Case 1

When the data is represented by region B, the best signal point must be one of the intersections of the ISI circle and the diagonals of the region because any other point on the circle will be closer to the boundaries of the region (i.e., corresponding to a smaller worst case noise margin), as shown in Fig. 14. From the figure, it can be seen that point c, which is not an intersection of the ISI circle and the diagonals, is always closer to the boundary than either intersection point a or b. The intersections a and b are compared in order to find the one with the largest worst case noise margin as the best signal point. That is, in Fig. 14, point b is chosen. With the truncated ISI (x_I, y_I), the equation for the ISI circle is

$$(x - x_I)^2 + (y - y_I)^2 = A^2. \tag{27}$$

The equations for the diagonals of region B are

$$y - x = 0 \quad \text{and} \quad x + y = 2L, \qquad \text{for } x, y \in [0, 2L). \tag{28}$$

The coordinates of all possible intersections are

$$x_1 = y_1 = \frac{x_I + y_I + \sqrt{(x_I + y_I)^2 - 2(x_I^2 + y_I^2 - A^2)}}{2} \tag{29}$$

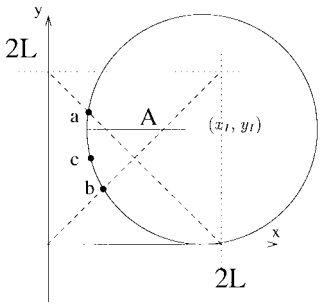

Fig. 14. Worst case noise margin of points on ISI circle.

$$x_2 = y_2 = \frac{x_I + y_I - \sqrt{(x_I + y_I)^2 - 2(x_I^2 + y_I^2 - A^2)}}{2} \tag{30}$$

and (31), given at the bottom of the page, and

$$y_3 = 2L - x_1 \tag{32}$$

and (33), given at the bottom of the page, and

$$y_4 = 2L - x_2 \tag{34}$$

and the one that gives the minimum value of $|x_i - L|, i = 1, 2, 3, 4$ (which implies that the point is closest to the center of the region and therefore has the largest worst case noise margin) will be chosen as the best signal point.

B. Case 2

When the data is represented by region C, there are two regions that may be used. The one closer to the ISI is chosen because the ISI circle goes deeper into that region than into the other, and, consequently, the best signal point in that region should have a larger worst case noise margin. That is, if the truncated ISI is in the left half of region B, the region C on the left will be chosen, otherwise, the one on the right will be chosen. Different from Case 1, the best signal point may or may not be one of the intersections of the ISI circle and the diagonals of the chosen C region. In Fig. 15, the left half of region B is divided into two subregions B_1 and B_2. If the ISI lies inside B_1, the best signal point will be one of the intersections, otherwise, the best signal point will be on the horizontal left of the truncated ISI and the phase of the precoded signal will be π. The reason is that in the first situation, the ISI circle intersects the diagonal(s) at an outgoing slope (going away from the center of the region) as shown in Fig. 16, and any other point on the circle is closer to the

$$x_3 = \frac{x_I - y_I + 2L + \sqrt{(x_I - y_I + 2L)^2 - 2(x_I^2 + (2L - y_I)^2 - A^2)}}{2} \tag{31}$$

$$x_4 = \frac{x_I - y_I + 2L - \sqrt{(x_I - y_I + 2L)^2 - 2(x_I^2 + (2L - y_I)^2 - A^2)}}{2} \tag{33}$$

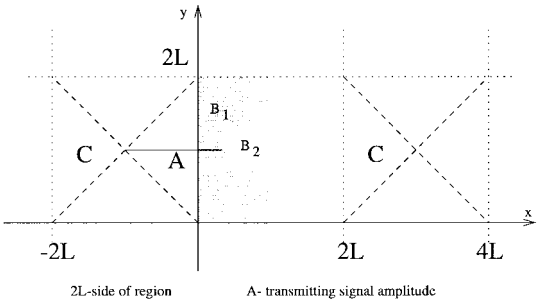

Fig. 15. Subregions in Case 2.

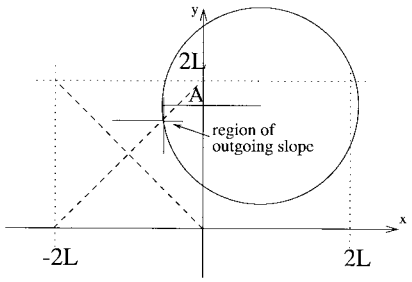

Fig. 16. ISI circle intersecting diagonals at outgoing slopes.

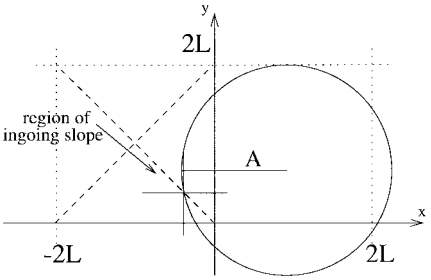

Fig. 17. ISI circle intersecting diagonals at ingoing slopes.

boundaries corresponding to a smaller worst case noise margin. On the other hand, when the truncated ISI lies in B_2, the ISI circle intersects the diagonals at an ingoing slope (getting closer to the center of the region) as shown in Fig. 17, and the intersections are not the closest points to the center of the region. The best signal point now should be the point with a noningoing slope (i.e., vertical slope) on the ISI circle, which is on the horizontal left of the truncated ISI.

When the truncated ISI is in subregion B_1, the best signal point can be determined by finding the roots of (27) and the equations for the diagonals of the left region C, which are

$$y+x=0 \quad \text{and} \quad y-x=2L, \quad \text{for } x\in[-2L,0), y\in[0,2L). \tag{35}$$

We can apply the results in Case 1 by shifting the coordinates of the truncated ISI to right by one region. Therefore, we replace (x_I, y_I) by (x_I+2L, y_I) in (34) and compare for the minimum $|x_i - L|$ value to find the best signal point. In particular, when the truncated ISI is in the lower left quarter of region B, the coordinates of the best signal point are

$$x=-y=\frac{x_I-y_I-\sqrt{(x_I+y_I)^2-2(x_I^2+y_I^2-A^2)}}{2}. \tag{36}$$

It should be noted that x is negative and y is positive. When the truncated ISI is in subregion B_2, the coordinates of the best signal point are

$$x=x_I-A \quad y=y_I. \tag{37}$$

The boundary between B_1 and B_2 is the locus of the truncated ISI that will have the same best signal point no matter whether the truncated ISI lies in B_1 or B_2, which are defined by

$$\begin{cases} y+x=A, & y\in[A-L,L] \\ y-x=2L-A, & y\in[L,3L-A] \end{cases} \tag{38}$$

for $A-L\le x\le L$. If the ISI lies in the right half of region B, the operation will be similar except that it should be a mirror image about $x=L$ of the above.

C. Cases 3 and 4

The cases when the data is represented by regions D and E are similar, except that one is the mirror image of the other about $y=L$. Therefore, here we only consider the case when the data is represented by region D. There are three D regions that may be used. Obviously, when the ISI lies in the left half of region B, the lower right region D should not be chosen. To choose from the remaining two D regions, we have to compare the best signal point attainable in the two regions for the better one. In Fig. 18, the left half of region B is divided into three subregions B_1', B_2', and B_3'. If the truncated ISI lies in subregions B_1' and B_3', the region D above region B should be selected. The best signal point is then found in a way similar to that in Case 2. That is, when the truncated ISI is in B_1', the best signal point is on the diagonal of the chosen region D, otherwise, the best signal point will be vertically above the truncated ISI and the phase of the precoded signal will be $\pi/2$. On the other hand, if the truncated ISI lies in region B_2', the lower left region D should be used. The best signal point should be on one diagonal of that region because the ISI circle always intersects with the diagonal(s) of that region at an outgoing slope.

As in Case 2, when the best signal point is on the diagonal of a region, we can apply the results of Case 1 by shifting the truncated ISI appropriately. That is, if the truncated ISI is in subregion B_1', we replace (x_I, y_I) with (x_I, y_I-2L) in (34); if the truncated ISI is in subregion B_2', we replace (x_I, y_I) with (x_I+2L, y_I+2L). The roots are then compared for the minimum $|x_i - L|$ value. The boundary between B_1' and B_3' is determined in a way similar to that of Case 2, and the corresponding equation is

$$y-x=2L-A, \qquad \text{for } x_0\le x\le L \tag{39}$$

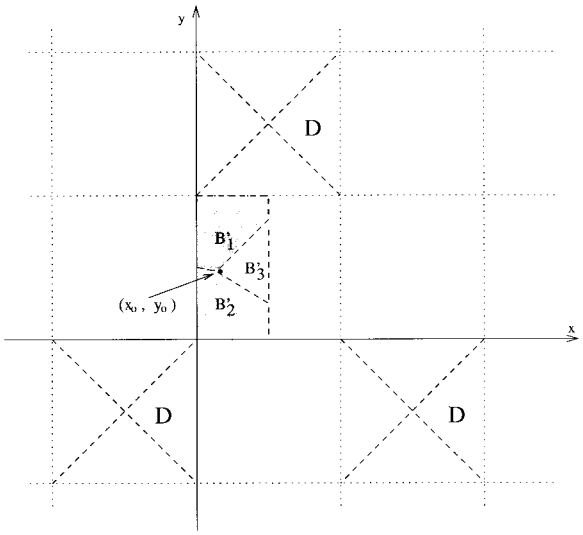

Fig. 18. Subregions in Case 3.

where (x_0, y_0) is the intersection of the three boundaries separating B'_1, B'_2, and B'_3. The boundary between B'_1 and B'_2 is found by assuming an truncated ISI belonging to B'_1 and B'_2 in turn and calculating the accessible largest worst case noise margin. If the results are the same, then the locus of the assumed ISI is the boundary needed. If the ISI is on that boundary, the ISI circle should intersect the diagonals

$$y - x = 2L, \qquad \text{for } x \in [0, 2L) \quad \text{and} \quad y \in [2L, 4L) \tag{40}$$

in the upper region D and

$$y - x = 0, \qquad \text{for } x, y \in [-2L, 0) \tag{41}$$

in the lower left region D. The coordinates of the intersections are

$$\begin{aligned} x_1 &= [x_I + y_I - 2L + \sqrt{2A^2 - (x_I - y_I + 2L)^2}]/2 \\ y_1 &= 2L + x_1 \end{aligned} \tag{42}$$

and

$$\begin{aligned} x_2 &= [x_I + y_I - \sqrt{2A^2 - (x_I - y_I)^2}]/2 \\ y_2 &= x_2 \end{aligned} \tag{43}$$

respectively. With the same worst case noise margin, we have $x_1 = -x_2$ and the equation for the boundary between B'_1 and B'_2 is

$$\begin{aligned} &(x^2 + y^2 - A^2)(y + x - L)^2 \\ &\quad + 2(x + y)(y + x - L)(L^2 - Ly) + 2(L^2 - Ly)^2 = 0. \end{aligned} \tag{44}$$

The same procedures can be applied to find the boundary between B'_2 and B'_3. If the truncated ISI is in region B'_3, the coordinates of the best signal point are

$$x = x_I \quad y = y_I + A \tag{45}$$

and the worst case noise margin is equal to $y_I + A - 2L$. Equating the worst case noise margins, the boundary between B'_2 and B'_3 is found to be

$$\begin{aligned} &x^2 + 5y^2 + 2xy + 2(A - 2L)x + 6(A - 2L)y + 8L^2 \\ &\quad - 8AL + A^2 = 0. \end{aligned} \tag{46}$$

The coordinates of the intersection of the three boundaries (x_0, y_0) can then be derived as

$$\begin{aligned} x_0 &= (A - 2L + \sqrt{A^2 + 4AL - 4L^2})/4 \\ y_0 &= (6L - 3A + \sqrt{A^2 + 4AL - 4L^2})/4. \end{aligned} \tag{47}$$

REFERENCES

[1] W. Zhuang, W. A. Krzymien, and P. A. Goud, "Trellis-coded CPFSK and soft-decision feedback equalization for micro-cellular wireless applications," *Wireless Personal Commun.*, vol. 1, no. 4, pp. 271–285, Oct. 1995.

[2] E. Dahlman, "Adaptive decision-feedback equalizers for fast-varying mobile-radio channels," Rep. TRITA-TTT-8912, Dec. 1989.

[3] S. U. H. Qureshi, "Adaptive equalization," *Proc. IEEE*, vol. 73, pp. 1349–1387, Sept. 1985.

[4] K. Wesolowski, "Efficient digital receiver structure for trellis-coded signals transmitted through channels with intersymbol interference," *Electron. Lett.*, vol. 23, no. 24, pp. 1265–1266, Nov. 1987.

[5] M. V. Eyuboglu and S. U. H. Qureshi, "Reduced-state sequence for coded modulation on intersymbol interference channels," *IEEE J. Select. Areas Commun.*, vol. 7, pp. 989–995, Aug. 1989.

[6] M. Tomlinson, "New automatic equalizer employing modulo-arithmetic," *Electron. Lett.*, vol. 7, pp. 138–139, Mar. 1971.

[7] H. Harashima and H. Miyakawa, "Matched-transmission technique for channels with intersymbol interference," *IEEE Trans. Commun.*, vol. COM-20, pp. 774–780, Aug. 1972.

[8] W. Zhuang, W. A. Krzymien, and P. A. Goud, "Adaptive channel precoding for personal communications," *Electron. Lett.*, vol. 30, pp. 1570–1571, Sept. 1994.

[9] W. Zhuang and V. W. Huang, "Phase precoding for frequency-selective Rayleigh and Rician slowly fading channels," *IEEE Trans. Veh. Technol.*, vol. 46, pp. 129–142, Feb. 1997.

[10] C. A. Balanis, *Antenna Theory: Analysis and Design*. New York: Harper, 1982, ch. 3.

[11] D. K. Cheng, *Field and Wave Electromagnetics*. Reading, MA: Addison-Wesley, 1991.

[12] H. Hashemi, "The indoor radio propagation channel," *Proc. IEEE*, vol. 81, pp. 943–967, July 1993.

[13] A. A. M. Saleh and R. A. Valenzuela, "A statistical model for indoor multipath propagation," *IEEE J. Select. Areas Commun.*, vol. SAC-5, pp. 128–137, Feb. 1987.

[14] T. A. Wilkinson, "Channel modeling and link simulation studies for the DECT test bed program," in *Proc. 6th IEE Int. Conf. Mobile Personal Commun.*, Coventry, U.K., 1991, pp. 293–299.

[15] J. Proakis, *Digital Communications*, 3rd ed. New York: McGraw-Hill, 1995.

[16] D. C. Cox, "Universal digital portable radio communications," *Proc. IEEE*, vol. 75, pp. 436–477, Apr. 1987.

[17] Y.-L. Chan, "Channel precoding with constant amplitude for QPSK over slowly fading channels using dimension partitioning technique," MA.Sc. thesis, Univ. Waterloo, Waterloo, Ont., Canada, Dec. 1995.

[18] S. Haykin, *Adaptive Filter Theory*. Englewood Cliffs, NJ: Prentice-Hall, 1986.

[19] G. J. Pottie and M. V. Eyuboglu, "Combined coding and precoding for PAM and QAM HDSL systems," *IEEE J. Select. Areas Commun.*, vol. 9, pp. 861–870, Aug. 1991.

[20] M. V. Eyuboglu and G. D. Forney, Jr., "Trellis precoding: Combined coding, precoding and shaping for intersymbol interference channels," *IEEE Trans. Inform. Theory*, vol. 38, pp. 301–314, Mar. 1992.

[21] *Cellular System Dual-Mode Mobile Station—Base Station Compatibility Standard (IS-54)*, EIA/TIA Interim Standard, Electronic Industries Association (EIA), May 1990.

[22] G. Ungerboeck, "Trellis-coded modulation with redundant signal sets. Part I & Part II," *IEEE Commun. Mag.*, vol. 25, pp. 5–21, Feb. 1987.

[23] D. D. Falconer, "Jointly adaptive equalization and carrier recovery in two-dimensional digital communication systems," *Bell Syst. Tech. J.*, pp. 317–334, Mar. 1976.

Yuk-Lun Chan received the B.Eng. degree in 1993 from the University of Hong Kong, Hong Kong, and the M.A.Sc. degree in 1996 from the University of Waterloo, Waterloo, Ont., Canada, both in electrical engineering.

He is now with the Delrina Group of Symantec Corporation as a Software Engineer. His research interests include digital transmission over fading dispersive channels, protocol implementation, and development for wireless communications.

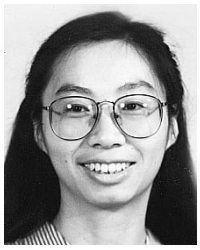

Weihua Zhuang (M'93) received the B.Sc. degree in 1982 and the M.Sc. degree in 1985, both from Dalian Marine University, China, and the Ph.D. degree in 1993 from the University of New Brunswick, Canada, all in electrical engineering.

Since 1993, she has been a Faculty Member at the University of Waterloo, Waterloo, Ont., Canada, where she is currently an Associate Professor in the Department of Electrical and Computer Engineering. Her current research interests include digital transmission over fading dispersive channels and wireless networking for multimedia personal communications.

Dr. Zhuang is a licensed Professional Engineer in the Province of Ontario, Canada.